

Gamow shell model description of the radiative capture reaction ${}^8\text{B}(p, \gamma){}^9\text{C}$

G.X. Dong,¹ X.B. Wang,¹ N. Michel,² and M. Płoszajczak^{3,*}

¹*School of Science, Huzhou University, Huzhou 313000, China*

²*Institute of Modern Physics, Chinese Academy of Sciences, Lanzhou, Gansu 730000, China*

³*Grand Accélérateur National d'Ions Lourds (GANIL),
CEA/DSM - CNRS/IN2P3, BP 55027, F-14076 Caen Cedex, France*

(Dated: December 27, 2022)

Background: In low metallicity supermassive stars, the hot pp chain can serve as an alternative way to produce the CNO nuclei. In the astrophysical environment of high temperature, the proton capture of ${}^8\text{B}$ can be faster than its beta decay, thus ${}^8\text{B}(p, \gamma){}^9\text{C}$ reaction plays an important role in the hot pp chain. Due to the unstable nature of ${}^8\text{B}$ and the lack of the ${}^8\text{B}$ beam, the measurement of ${}^8\text{B}(p, \gamma){}^9\text{C}$ reaction can only be achieved by the indirect method, and large uncertainties exist.

Purpose: The Gamow shell model in the coupled-channel representation (GSM-CC) is applied to study the proton radiative capture reaction ${}^8\text{B}(p, \gamma){}^9\text{C}$.

Method: The GSM-CC is a unified microscopic theory for the description of nuclear structure and nuclear reaction properties. The translationally invariant Hamiltonian is adopted with a finite-range two-body interaction, the parameters of which are adjusted to reproduce the low-energy spectra of ${}^8\text{B}$ and ${}^9\text{C}$. The reaction channels are then built through the coupling of the wave functions of the ground state 2_1^+ , the first excited state 1_1^+ , and the second excited state 3_1^+ in ${}^8\text{B}$ with the proton wave function in different partial waves. For the calculation of the ${}^8\text{B}(p, \gamma){}^9\text{C}$ astrophysical factors, all E1, M1, and E2 transitions from the initial continuum states to the final bound states $3/2_1^-$ of ${}^9\text{C}$ are considered. The resonant capture to the first resonant state $1/2_1^-$ of ${}^9\text{C}$ is also calculated.

Results: The experimental low-energy levels and the proton emission threshold in ${}^9\text{C}$ are reproduced by the GSM-CC. The calculated astrophysical factors agrees with the existed experimental data from the indirect measurements. The reaction rates from the direct capture and resonant capture are calculated for the temperature range of astrophysical interest.

Conclusion: The calculated total astrophysical S factor is dominated by the E1 transition to the ground state of ${}^9\text{C}$. The GSM-CC calculations suggest that S first increase with the energy of the center of mass $E_{\text{c.m.}}$, and then decrease with the energy. This agrees with the existing data, which has smaller values at around zero energy and larger value in the energy range of $0.2 \text{ MeV} \leq E_{\text{c.m.}} \leq 0.6 \text{ MeV}$.

PACS numbers: 03.65.Nk, 31.15.-p, 31.15.V-, 33.15.Ry

I. INTRODUCTION

The nucleosynthesis of light nuclei is hindered by the mass gap of $A=8$, where no stable nuclei exist. However, this gap can be overcome in some astrophysical sites. It is well known that the radiative proton capture reaction ${}^8\text{B}(p, \gamma){}^9\text{C}$ plays an important role in the hot proton-proton chain in low-metallicity supermassive stars [1, 2]. If the density is sufficiently high ($\geq 2 \times 10^7 \text{ g/cm}^3$) and the temperature is in the range $0.07 \leq T_9 \leq 0.7$, the proton capture and the alpha capture can be faster than the beta decay [1]. Thus, this reaction can serve as an alternative way to the three alpha process to form the CNO nuclei, through the reaction chain as: ${}^7\text{Be}(p, \gamma){}^8\text{B}(p, \gamma){}^9\text{C}(\alpha, p){}^{12}\text{N}(p, \gamma){}^{13}\text{O}(\beta^+){}^{13}\text{N}(p, \gamma){}^{14}\text{O}$ [1].

The charge particle capture cross section is hindered by the Coulomb repulsion. Because of the very small reaction cross section, and low intensity of the ${}^8\text{B}$ beam, the direct measurement of ${}^8\text{B}(p, \gamma){}^9\text{C}$ reaction is difficult if not impossible. There are usually two different ways of indirect measurements of this reaction. One is through

the asymptotic normalization coefficients (ANC) for the virtual decay and then the astrophysical S factor can be deduced. The other is the Coulomb-dissociation experiment by the radioactive beams.

There are several experimental studies concerning ${}^8\text{B}(p, \gamma){}^9\text{C}$ reaction based on the ANC method. Beaumel et al. measured ${}^8\text{B}(d, n){}^9\text{C}$ reaction cross section in the inverse kinematics at 14.4 MeV/u and derived the ANC of the virtual decay of ${}^9\text{C} \rightarrow {}^8\text{B} + p$ using the distorted-wave Born approximation (DWBA) [3]. A similar analysis has been performed later at $E_{\text{c.m.}}=7.8 \text{ MeV}$ by Guo et al. [4].

Trache et al. investigated the breakup of ${}^9\text{C}$ at intermediate energies to extract the ANC and derive the astrophysical S factor using the Glauber model [5]. Recently, this experiment was re-analyzed using the continuum discretized-coupled-channel (CDCC) approach and the eikonal reaction theory (ERT) [6]. The value of $S(0)$ obtained in this analysis was found larger by about 43% than previously reported [5].

Based on the CDCC approach, Fukui et al. re-analyzed also the ${}^8\text{B}(d, n){}^9\text{C}$ measurement [3], and got a smaller value of the S factor than obtained in the DWBA analysis [7].

Finally, Motobayashi determined the S factor of the

* ploszajczak@ganil.fr

${}^8\text{B}(p, \gamma){}^9\text{C}$ reaction in the Coulomb dissociation experiment, in which ${}^9\text{C}$ bombards the lead target and is Coulomb excited to an unbound state that decays in the ${}^8\text{B}+p$ channel [8]. The S factor in the energy range $0.2 \text{ MeV} \leq E_{\text{c.m.}} \leq 0.6 \text{ MeV}$ reported in this analysis is significantly larger than found in all other experimental analyses of the S factor at $E_{\text{c.m.}}=0$ [3–7, 9].

Theoretical calculations of the S factor in the ${}^8\text{B}(p, \gamma){}^9\text{C}$ reaction exhibit large discrepancies. Based on the nuclear structure information, a very large value of $S(0)$ ($\sim 210 \text{ eV barn}$) was obtained in a simple potential model [1]. Studies of the ${}^8\text{B}(p, \gamma){}^9\text{C}$ reaction using the microscopic cluster model showed a significant dependence of the S factor on the chosen potential [10, 11]. Mirror reactions ${}^8\text{Li}(n, \gamma){}^9\text{Li}$ and ${}^8\text{B}(p, \gamma){}^9\text{C}$ were studied by P. Mohr using the direct capture model [12]. It was found that the cross sections depend strongly on chosen parameters of the potential which could be explained by the resonant states in the potential model.

In this paper, we focus on the study of the proton radiative capture reaction ${}^8\text{B}(p, \gamma){}^9\text{C}$ in a general framework of the Gamow shell model (GSM) [13–18]. In this model, the many-body states are described as a linear combination of Slater determinants composed by the single-particle (s.p.) bound, resonant and non-resonant scattering states of the Berggren ensemble [19]. The GSM is an excellent tool for the nuclear structure studies. However, in the Slater determinant representation there is no separation between different reactions channels. Hence, the direct application of the GSM for nuclear reactions is not possible. This problem can be solved by formulating GSM in the coupled-channel representation (GSM-CC) [16, 18, 20, 21]. In this representation, one obtains the unified theory of nuclear structure and reactions which was applied to several reaction studies, e.g., the low-energy elastic and inelastic proton scattering [16], deuteron elastic scattering [22], and the radiative capture reactions [17, 23, 24].

This paper is organized as follows. The formalism of GSM-CC is briefly introduced in Sec. II. Results of GSM-CC calculation are presented and discussed in Sec. III. In this section, the low-energy spectrum of ${}^8\text{B}$ and ${}^9\text{C}$ is given in Sec. III A and the low-energy astrophysical factor of ${}^8\text{B}(p, \gamma){}^9\text{C}$ reaction is studied in Sec. III B. The astrophysical reaction rates are discussed in Sec. III C. Finally, the summary and main conclusions are given in Sec. IV.

II. THE GAMOW SHELL MODEL IN THE COUPLED-CHANNEL REPRESENTATION

In this section, we briefly introduce the GSM-CC approach. For a complete presentation of the formalism, reader can refer to Refs. [15, 18] and references cited therein.

In GSM, the Hamiltonian in the intrinsic nucleon-core coordinates of the cluster-orbital shell model (COSM) is

used to remove the spurious center of mass (c.m.) excitations in the wave function [25]:

$$\hat{H} = \sum_{i=1}^{N_{\text{val}}} \left(\frac{\hat{\vec{p}}_i^2}{2\mu_i} + U_{\text{core}}(\hat{\vec{r}}_i) \right) + \sum_{i < j}^{N_{\text{val}}} \left(V(\hat{\vec{r}}_i - \hat{\vec{r}}_j) + \frac{\hat{\vec{p}}_i \cdot \hat{\vec{p}}_j}{M_{\text{core}}} \right), \quad (1)$$

in which N_{val} stands for the valence particle number, M_{core} is the mass of the core, μ_i indicates the reduced mass of the proton or neutron, and $U_{\text{core}}(\hat{\vec{r}})$ denotes the s.p. potential of the core acting on each of the valence nucleons. $V(\hat{\vec{r}}_i - \hat{\vec{r}}_j)$ is the two-body interactions between valence nucleons, which is translationally invariant. In the above formula, the last term is the recoil term [18].

The A -body system is decomposed into reaction channels, as

$$|\Psi_M^J\rangle = \sum_c \int_0^{+\infty} |(c, r)_M^J\rangle \frac{u_c^{JM}(r)}{r} r^2 dr, \quad (2)$$

where $u_c^{JM}(r)$ is the radial amplitude describing the relative motion between the target and projectile in channel c . It is obtained by solving the GSM coupled-channel equations for the given total angular momentum J and its projection M . The variable r in the above equation denotes the relative distance between the c.m. of the target and the projectile. $|(c, r)_M^J\rangle$ is the binary-cluster channel state defined as:

$$|(c, r)_M^J\rangle = \hat{\mathcal{A}} |\{\Psi_{\text{T}}^{J_{\text{T}}}\}\rangle \otimes |\Psi_{\text{p}}^{J_{\text{p}}}\}_M^J\rangle. \quad (3)$$

The channel index c indicates the mass partitions and quantum numbers. $\hat{\mathcal{A}}$ stands for the antisymmetrizations among nucleons belonging to different clusters. $|\Psi_{\text{T}}^{J_{\text{T}}}\rangle$ and $|\Psi_{\text{p}}^{J_{\text{p}}}\rangle$ are the target and projectile states with their angular momentum J_{T} and J_{p} , respectively. The coupling of J_{T} and J_{p} leads to the total angular momentum J .

Starting from the Schrödinger equation, the coupled-channel equation can be derived as

$$\oint_c \int_0^{\infty} dr r^2 (H_{c',c}(r', r) - EO_{c',c}(r', r)) \frac{u_c(r)}{r} = 0, \quad (4)$$

where E stands for the scattering energy of the A -body system, and the kernels are the Hamiltonian and the norm matrix elements in the channel representation, respectively, as

$$H_{c',c}(r', r) = \langle r', c' | \hat{H} | r, c \rangle, \quad (5)$$

and

$$O_{c',c}(r', r) = \langle r', c' | r, c \rangle. \quad (6)$$

The channel state $|r, c\rangle$ can be built from a complete Berggren s.p. basis [19] containing the bound, resonant,

and non-resonant scattering states from the contour in the complex k -plane [13–15, 18]:

$$|r, c\rangle = \sum_i \frac{u_i(r)}{r} |\phi_i^{\text{rad}}, c\rangle, \quad (7)$$

in which $|\phi_i^{\text{rad}}, c\rangle = \hat{\mathcal{A}}(|\phi_i^{\text{rad}}\rangle \otimes |c\rangle)$, $u_i(r)/r = \langle \phi_i^{\text{rad}} | r \rangle$, and $|\phi_i^{\text{rad}}\rangle$ is the radial part. The channel basis states $|r, c\rangle$ are nonorthogonal, which is caused by the antisymmetrization between projectile and target states. The orthogonal channel basis states ($|r, c\rangle_o = \hat{O}^{-\frac{1}{2}} |r, c\rangle$) can be obtained from

$$_o \langle r', c' | r, c \rangle_o = \frac{\delta(r' - r)}{r^2} \delta_{c'c} \quad (8)$$

where \hat{O} is the overlap operator. Then, the GSM-CC equation (4) is derived as:

$$\oint_c \int_0^\infty dr r^2 ({}_o \langle r', c' | \hat{H}_o | r, c \rangle_o - E_o \langle r', c' | \hat{O} | r, c \rangle_o) \times {}_o \langle r, c | \Psi_o \rangle = 0, \quad (9)$$

in which $\hat{H}_o = \hat{O}^{\frac{1}{2}} \hat{H} \hat{O}^{\frac{1}{2}}$, and $|\Psi_o\rangle = \hat{O}^{1/2} |\Psi\rangle$.

Assuming $|\Phi\rangle = \hat{O} |\Psi\rangle$, the generalized eigenvalue problem given in Eq. (9) is transformed into a standard equation:

$$\oint_c \int_0^\infty dr r^2 ({}_o \langle r', c' | \hat{H} | r, c \rangle_o - E_o \langle r', c' | r, c \rangle_o) {}_o \langle r, c | \Phi \rangle = 0. \quad (10)$$

With the nonorthogonal channel basis states, the coupled-channel equation becomes:

$$\oint_c \int_0^\infty dr r^2 \langle r', c' | \hat{H}_m | r, c \rangle \frac{w_c(r)}{r} = E \frac{w_{c'}(r')}{r'}, \quad (11)$$

where $\hat{H}_m = \hat{O}^{-\frac{1}{2}} \hat{H} \hat{O}^{-\frac{1}{2}}$ and

$$w_c(r)/r \equiv \langle r, c | \hat{O}^{\frac{1}{2}} | \Psi \rangle = {}_o \langle r, c | \Phi \rangle.$$

Because of the completeness of the Berggren basis, these coupled-channel equations (11) can be solved numerically from the Berggren basis expansion of the Green's function $(H - E)^{-1}$, details of which have been explained in Refs. [18, 22].

III. DISCUSSION AND RESULTS

In GSM and GSM-CC calculations we assume ${}^4\text{He}$ as the inert core. The core potential in the Hamiltonian is given by the Woods-Saxon (WS) potential with the spin-orbit term (see Table I). As an interaction, the Furutani-Horiuchi-Tamagaki (FHT) finite-range two-body force is used [26, 27]. Parameters of this interaction are adjusted

to reproduce energies of low-lying states and proton separation energies in ${}^8\text{B}$ and ${}^9\text{C}$ (see the Table II).

In GSM-CC, the two-body Hamiltonian from which the channel-channel coupling potentials are calculated, is usually re-scaled by the small multiplicative corrective factors $c(J^\pi)$ for $J^\pi = 3/2^-_1, 1/2^-_1, 5/2^-_1$ states. They are used to compensate for missing correlations in the GSM-CC wave function, due to the neglecting of non-resonant channels built by coupling the continuum states of ${}^8\text{B}$ with the proton projectile in different partial waves. The corrective factors used in this work are: $c(3/2^-) = 1.026, c(1/2^-) = 1.1, c(5/2^-) = 1.0286$. Detailed discussions of the FHT interaction in the application of GSM can be found in Refs. [17, 23, 28].

Let us comment on the physical properties of the used FHT parameters of Table II. By considering the singular values associated to the correlation matrix used in the fitting procedure, one can identify the well fitted and sloppy FHT parameters [18, 28]. In our present case, the $\nu_{s,t}^C$ and $\nu_{t,s}^C$ parameters are well defined, as they bear the largest singular values. Conversely, $\nu_{t,t}^{SO}$ and $\nu_{t,t}^T$ are the most sloppy parameters, as they can be associated to the smallest singular values, close to zero. Remaining parameters, i.e. $\nu_{t,t}^C$, $\nu_{s,s}^C$, $\nu_{t,t}^T$ and $\nu_{s,t}^T$, are mildly important as their associated singular values lie in between. This is consistent with the analysis done in Ref.[28], where fitted FHT parameters qualitatively present similar singular values. Consequently, even though the FHT interaction had to be hereby refitted as the model spaces of Ref.[28] and of this paper are different, both interactions possess the same statistical properties, so that they can be considered to be of the same quality from a physical point of view.

TABLE I. Parameters of the WS potential of ${}^4\text{He}$ core which are used in the description of ${}^8\text{B}$, ${}^9\text{C}$ spectra, and proton-capture cross-section ${}^8\text{B}(p, \gamma){}^9\text{C}$. The radius of Coulomb potential r_{Coul} equals 2.54 fm.

Parameter	Protons	Neutrons
a	0.650 fm	0.650 fm
R_0	2.000 fm	2.000 fm
$V_o(l=0)$	66.717 MeV	64.328 MeV
$V_o(l=1)$	44.546 MeV	63.974 MeV
$V_o(l=2)$	42.466 MeV	60.669 MeV
$V_{so}(l=1)$	8.500 MeV	8.500 MeV
$V_{so}(l=2)$	8.500 MeV	8.500 MeV

The Berggren ensemble for protons consists of two resonant s.p. states $0p_{3/2}$ and $0p_{1/2}$, 21 s.p. states in the non-resonant continuum along the contours $\mathcal{L}_{p_{1/2}}^+, \mathcal{L}_{p_{3/2}}^+$, and several scattering-like s.p. states $s_{1/2}$, $d_{3/2}$ and $d_{5/2}$. Each contour consists of three segments connecting the points: $k_{\text{min}}=0.0$, $k_{\text{peak}} = 0.15 - i0.10 \text{ fm}^{-1}$, $k_{\text{middle}}=0.3 \text{ fm}^{-1}$ and $k_{\text{max}}=2.0 \text{ fm}^{-1}$, and each segment is discretized with 7 points. For both $d_{3/2}$ and $d_{5/2}$ of scattering-like states, six harmonic oscillator states are taken, while for $s_{1/2}$ of scattering-like state, five harmonic oscillator states

TABLE II. Parameters of the FHT interaction in GSM and GSM-CC calculations. The superscripts C, SO, and T denote central, spin-orbit, and tensor, respectively. The indices "s" and "t" stand for singlet and triplet, respectively.

Parameter	Value
$\nu_{t,t}^C$	-1.669 MeV
$\nu_{s,t}^C$	-5.204 MeV
$\nu_{s,s}^C$	1.233 MeV
$\nu_{t,s}^C$	-4.019 MeV
$\nu_{t,t}^{SO}$	-1427.795 MeV
$\nu_{s,t}^{SO}$	0 MeV
$\nu_{t,t}^T$	53.442 MeV fm ⁻²
$\nu_{s,t}^T$	-22.284 MeV fm ⁻²

are taken. Each s.p. state of the Berggren ensemble becomes the shell in the many-body GSM and GSM-CC calculation. For neutrons, only $0p_{3/2}$ and $0p_{1/2}$ resonant s.p. states, and $1s_{1/2}$, $0d_{5/2}$ and $0d_{3/2}$ three harmonic oscillator states are taken. Thus, the GSM and GSM-CC calculations are performed in 61 shells for protons: 44 $p_{3/2}$ and $p_{1/2}$ shells, 17 $s_{1/2}$, $d_{3/2}$, and $d_{5/2}$ scattering-like shells, and 5 shells for neutrons: 2 shells $p_{3/2}$ and $p_{1/2}$, 3 scattering-like shells $s_{1/2}$, $d_{3/2}$, and $d_{5/2}$.

A. Energy spectrum of ^8B and ^9C

For the GSM-CC calculation of $^8\text{B}(p, \gamma)^9\text{C}$ reaction, the first step is to calculate the low-lying states of the target nucleus ^8B by GSM. The channel states in GSM-CC are then built by coupling three states of ^8B , i.e., the ground state $J_T^\pi = 2_1^+$, the first and the second excited states, $J_T^\pi = 1_1^+$ and $J_T^\pi = 3_1^+$, which are both low-lying resonances, with the proton in partial waves: $s_{1/2}$, $p_{1/2}$, $p_{3/2}$, $d_{3/2}$ and $d_{5/2}$. For ^8B in the GSM calculation, there is no truncation, which means that all valence particles can occupy the scattering and scattering-like shells without any restriction. For ^9C in the GSM-CC calculation, due to the huge dimension of the Fock space, we truncated the basis of Slater determinants by limiting the occupation of scattering shells and scattering-like shells up to three particles.

The GSM energies and width of the low-lying states of ^8B are given in Fig. 1 (a), together with the experimental data. The GSM-CC energies and widths of ^9C states as well as the proton separation energy are compared with the experimental data [29, 30] in Fig. 1 (b). Energies of levels relative to the ground state are listed in Table. III for ^8B and ^9C . The calculated ground-state energy of ^8B with respect to ^4He is -9.554 MeV, which is rather close to the experimental value -9.441 MeV [29]. The calculated energies and widths of the first and second excited states in ^8B are also fairly close to data.

To reach the high precision of calculated radiative capture reaction cross section, we use the experimental ground-state energy of ^8B in the coupled-channel equa-

tions. In this way, we ensure that the experimental proton separation energy in ^9C is used in the cross-section calculation. The calculated energies of low-lying states in ^9C , are close to the experimental data.

As seen in the figure, the first excited state of ^9C is a resonance. The experimental positive parity state $5/2_1^+$ is a very broad resonance, with the reported width $\Gamma = 2.750$ (110) MeV in Ref. [30], and $\Gamma = 4.0_{-1.4}^{+2.0}$ MeV in the more recent measurement [31]. In GSM-CC calculation, the energy of $5/2_1^+$ state is close to the experimental value but its width is smaller than in the data. The energy of the positive parity state, $3/2_1^+$, is very close to that of $5/2_1^+$. The resonance with unknown spin and parity in experimental data is predicted to be $1/2_1^+$ state.

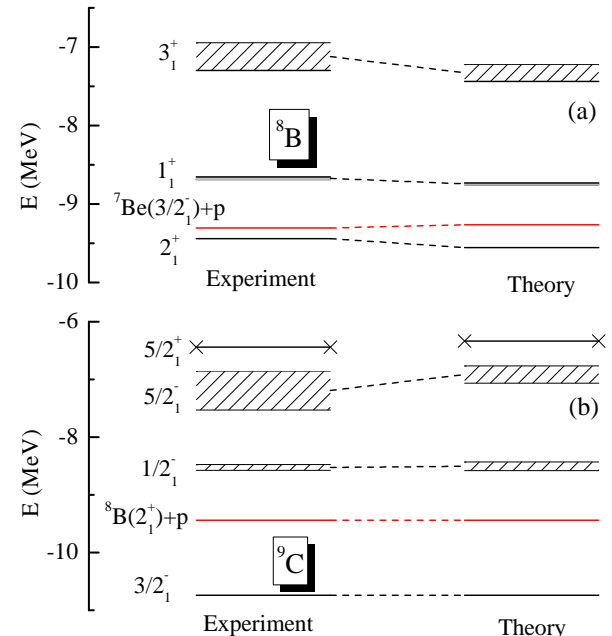


FIG. 1. GSM energy levels of ^8B and GSM-CC energy levels of ^9C are compared with the experimental data [29, 30] in panels (a) and (b), respectively. Energies are given relative to the energy of ^4He . The measured $5/2_1^+$ state has a very broad width which is not shown in the figure. For more details see Table III and a discussion in the text.

B. The astrophysical factor for $^8\text{B}(p, \gamma)^9\text{C}$ reaction

After the calculation of eigenfunctions of ^8B in GSM, the proton capture cross section to the final state of ^9C with the total angular momentum J_f can be obtained by an expression [18]:

$$\sigma_{J_f}(E_{\text{c.m.}}) = \int_0^{2\pi} d\varphi_\gamma \int_0^\pi \sin \theta_\gamma d\theta_\gamma \frac{d\sigma_{J_f}(E_{\text{c.m.}}, \theta_\gamma, \varphi_\gamma)}{d\Omega\gamma}, \quad (12)$$

where $E_{\text{c.m.}}$ is the center of mass energy of ^9C . The proton emission threshold in ^9C corresponds to $E_{\text{c.m.}} = 0$.

TABLE III. The calculated excitation energies of low energy bound and resonance states in ${}^8\text{B}$ and ${}^9\text{C}$ are compared with the experimental data. All energies are given relative to their respective ground states. The experimental data are taken from Refs. [29, 30].

	Theory		Experiment			
	J^π	$E(\text{MeV})$	$\Gamma(\text{keV})$	J^π	$E(\text{MeV})$	$\Gamma(\text{keV})$
${}^8\text{B}$	2_1^+	0.000	-	2_1^+	0.000	-
	1_1^+	0.811	24.89	1_1^+	0.7695(25)	35.6 (6)
	3_1^+	2.154	244.97	3_1^+	2.32(20)	350 (30)
${}^9\text{C}$	$3/2_1^-$	0.000	-	$3/2_1^-$	0.000	-
	$1/2_1^-$	2.236	147.88	$1/2_1^-$	2.218(11)	52(11)
	$5/2_1^-$	3.827	301.99	$5/2_1^-$	3.549(20)	673(50)
	$3/2_1^+$	4.375	328.35	$5/2_1^+$ ^a	4.40(4)	2750(110)
	$5/2_1^+$	4.401	327.63			
	$1/2_1^+$	5.928	367.57	?	5.75(4)	601(50)

^a The latest measured energy of $5/2_1^+$ is 4.3 (3) MeV, and width is $4.0^{+2.0}_{-1.4}$ [31].

The differential cross-sections $d\sigma_{J_f}/d\Omega\gamma$ in (12) are calculated from matrix elements of the electromagnetic operators between the antisymmetrized initial and final states of ${}^8\text{B}$ and ${}^9\text{C}$. The electromagnetic transitions connect the continuum states in ${}^9\text{C}$ with the final state, which can be the bound state $J_f = 3/2_1^-$ or the resonance $1/2_1^-$. We consider continuum states with $J_i = 1/2^+, 3/2^+, 5/2^+$ for the E1 transition, and continuum states with $J_i = 1/2^-, 3/2^-, 5/2^-$ for the M1 and $J_i = 1/2^-, 3/2^-, 5/2^-, 7/2^-$ for the E2 transition. The total cross section is the summation of σ_{J_f} with all possible J_f . Details of the cross-section calculation and the approximations used in the many-body matrix elements of the electromagnetic operators in GSM-CC approach can be found in Refs. [17, 18, 23].

To remove an exponential dependence of the cross section due to the Coulomb barrier, it is convenient to consider the astrophysical S factor instead of the radiative capture cross section for charged particles:

$$S(E_{\text{c.m.}}) = \sigma(E_{\text{c.m.}})E_{\text{c.m.}}e^{2\pi\eta}. \quad (13)$$

η in this expression is the Sommerfeld parameter $\eta = e^2 Z_1 Z_2 / \hbar \nu$.

For the calculation of E1 and E2 transitions, effective charges are used. For E1 transitions, the empirical effective charges [38, 39] are:

$$e_{\text{eff}}^p(\text{E1}) = e f_{\text{E1}} \left(1 - \frac{Z}{A}\right); \quad e_{\text{eff}}^n(\text{E1}) = -e f_{\text{E1}} \frac{Z}{A}, \quad (14)$$

where Z and A are the proton number and total particle number in the combined system of a target nucleus and a projectile. f_{E1} is the scaling factor. For $f_{\text{E1}} = 1.0$, the effective charges originate from the recoil correction of the center of mass [38, 39]. In the studies of the radiative neutron capture reactions using the valence capture model [40, 41], a broader range of neutron effective charges: $1 \leq f_{\text{E1}} < 3$ was suggested [39].

TABLE IV. The electric quadrupole and magnetic moments of the ground state of ${}^8\text{B}$ and ${}^9\text{C}$. The experimental electric quadrupole moment of ${}^8\text{B}$ is from Ref. [32]. The experimental data for the magnetic moment of ${}^8\text{B}$ and ${}^9\text{C}$ are from Ref. [33] and Ref. [34], respectively. The GSM calculations of electric quadrupole moment are done with different effective charges. For SM results, we show results of Huhta et al. [34]. Other SM calculations are done using OXBASH code [35] and the same p -shell interaction [36] as in Ref. [34]. For more details, see the description in the text.

	${}^8\text{B}, 2_1^+$	${}^9\text{C}, 3/2_1^-$
$Q(e^2 \text{fm}^2)$		
Experiment	+6.43(14)	
GSM (1.00e, 0.00e)	+2.029	-1.271
GSM (1.26e, 0.47e) [37]	+3.525	-3.017
GSM (recoil correction)	+1.841	-1.306
SM (1.00e, 0.00e)	+1.997	-1.401
SM (1.26e, 0.47e) [37]	+2.970	-2.593
SM (recoil correction)	+1.729	-1.324
$\mu(\mu_N)$		
Experiment	1.0355(3)	(-)1.396(3)
GSM	0.833	-1.114
SM	1.132	-1.438 [34]

In this work we use $f_{\text{E1}} = 1$ if not mentioned otherwise. For E2 transitions, the commonly-used values of the proton and the neutron effective charges are in the range of $1.1e < e_{\text{eff}}^p(\text{E2}) < 1.5e$ and $0.5e < e_{\text{eff}}^n(\text{E2}) < 0.6e$, respectively [37, 42–44]. For the calculation of M1 transitions, effective charges are not needed .

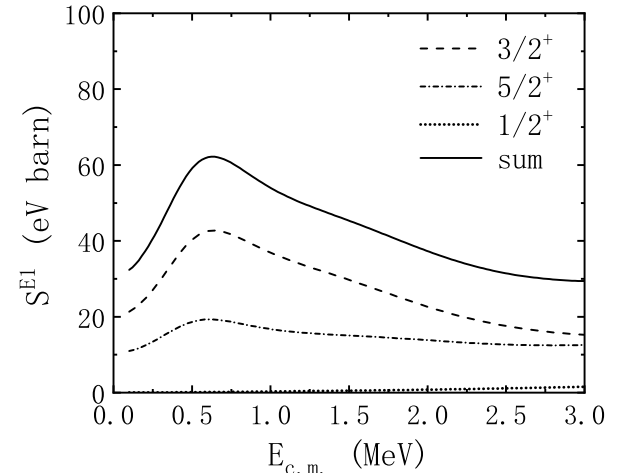


FIG. 2. The E1 astrophysical factor for the ${}^8\text{B}(p, \gamma){}^9\text{C}$ reaction is plotted as a function of the proton projectile energy in the $p + {}^8\text{B}$ center of mass frame. The solid line represents the fully antisymmetrized GSM-CC calculation for the radiative proton capture to the ground state of ${}^9\text{C}$. The dashed, dashed-dotted, and dotted lines show the contributions from the radiative proton capture to the ${}^9\text{C}$ ground state from the initial continuum states with $J_i^\pi = 3/2^+, 5/2^+$, and $1/2^+$, respectively.

$$e_{\text{eff}}^p(\text{E2}) = e \left(1 - \frac{2}{A} + \frac{Z}{A^2} \right); \quad e_{\text{eff}}^n(\text{E2}) = Z/A^2 e, \quad (15)$$

are labeled “recoil correction”. One may notice that large effective charge would be needed to reproduce the experimental quadrupole moment of ${}^8\text{B}$.

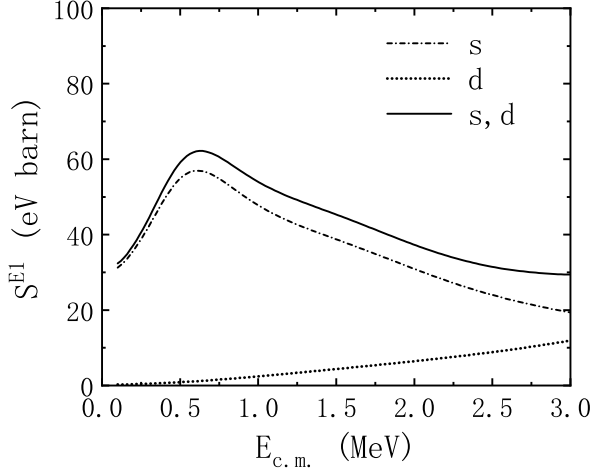


FIG. 3. The solid line shows the E1 astrophysical factor S^{E1} as a function of proton projectile energy in the $\text{p} + {}^8\text{B}$ center of mass frame for the proton radiative capture to the ground state of ${}^9\text{C}$. The E1 radiative capture of s - and d -wave protons is shown as the dashed-dotted and dotted lines, respectively.

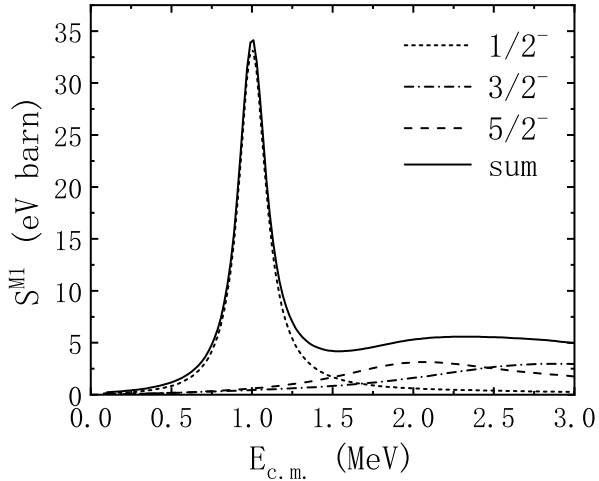


FIG. 4. The M1 astrophysical factor for the radiative proton capture to the ground state of ${}^9\text{C}$ is plotted by the solid line as a function of the proton projectile energy. The peak corresponds to the $1/2_1^-$ resonance of ${}^9\text{C}$. The dashed, dashed-dotted, and dotted lines show the contributions from the radiative proton capture to the ${}^9\text{C}$ ground state from the initial continuum states with $J_i^\pi = 1/2^-$, $3/2^-$, and $5/2^-$, respectively.

Figs. 2-5 show separate contributions to the total astrophysical S factor for the ${}^8\text{B}(p, \gamma){}^9\text{C}$ reaction to the ground state of ${}^9\text{C}$: S^{E1} for E1 transitions (Figs. 2 and

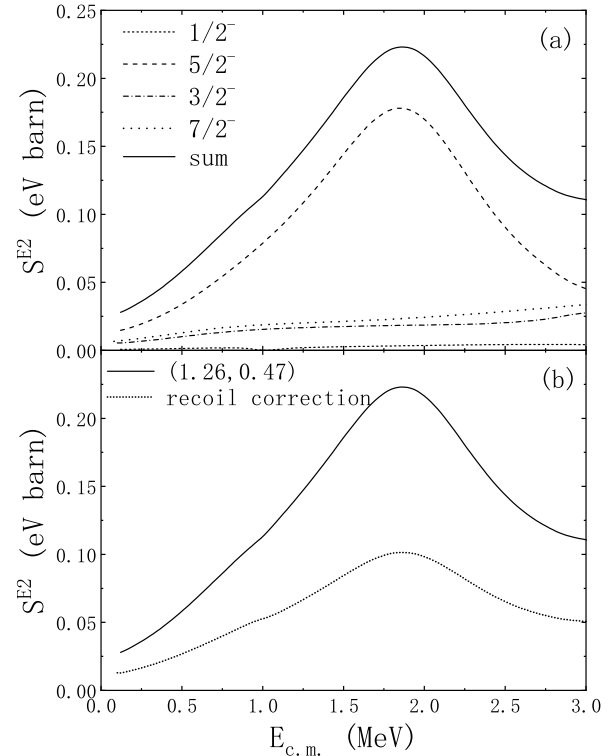


FIG. 5. The E2 astrophysical factor is plotted as a function of the proton projectile energy. In the upper panel (a), the solid line shows the sum of individual contributions of different initial continuum states $J_i^\pi = 3/2_1^-, 1/2_1^-, 5/2_1^-, 7/2_1^-$ to the astrophysical S^{E2} factor of the radiative proton capture to the ground state of ${}^9\text{C}$. The E2 effective charges $(e_{\text{eff}}^p, e_{\text{eff}}^n) = (1.26e, 0.47e)$ [37] are used. The lower panel (b) compares two different sets of E2 effective charges. The solid line is the same as in the panel (a). The dotted line is calculated for the E2 effective charges from the recoil of the center of mass (15).

3); S^{M1} for M1 transitions (Fig. 4); S^{E2} for E2 transitions (Fig. 5). The major contribution to the S factor comes from the E1 transitions. Especially, the capture of s -wave proton to the ground state of ${}^9\text{C}$ plays a crucial role, as seen in Fig. 3. This finding is also consistent with results of previous studies [4, 5, 12].

One can see in Fig. 2 that the values of S^{E1} first increase with $E_{\text{c.m.}}$ and then decrease, forming a broad bump at $E_{\text{c.m.}} \sim 0.6$ MeV. The largest contribution to S^{E1} comes from the initial continuum states $J_i^\pi = 3/2^+, 5/2^+$ which both exhibit a broad peak at around 0.6 MeV. The contribution of $J_i^\pi = 3/2^+$ continuum is larger than that from the $J_i^\pi = 5/2^+$. A similar conclusion was drawn in the studies using the microscopic cluster model [10, 11].

In Fig. 4 one can see a sharp peak for the M1 transition, which is caused by the $1/2_1^-$ resonance. The $1/2_1^-$ resonance lies above the one-proton decay threshold. The center-of-mass energy of this peak is: $E_{\text{c.m.}} = E_i^{(A)}[\text{GSM-CC}] - E_0^{(A-1)}[\text{GSM}]$, where $E_i^{(A)}[\text{GSM-CC}]$ is the GSM-CC energy of resonance i in ${}^9\text{C}$, and

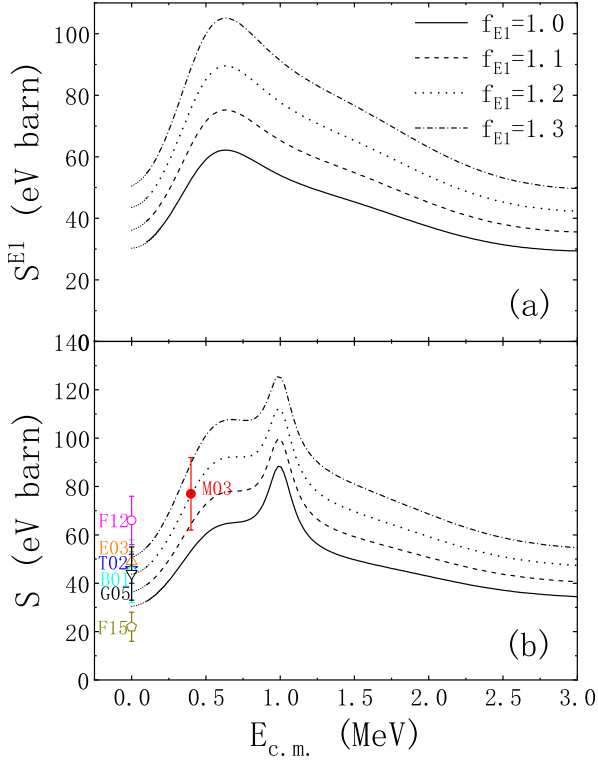


FIG. 6. Panel (a): the E1 astrophysical factor for the radiative proton capture to the ground state of ${}^9\text{C}$ is plotted as a function of the proton projectile energy for different values of the scaling factors f_{E1} of E1 effective charges (see Eq. (14)). The total astrophysical S factor is plotted in panel (b). Different lines correspond to the GSM-CC calculations using different f_{E1} values, and the same E2 effective charges (1.26e, 0.47e) [37]. Standard g-factors are used in M1 contribution S^{M1} . The astrophysical factor of the proton radiative capture reaction in the limit $E_{\text{c.m.}} \rightarrow 0$ has been extracted by using the expansion with a quadratic polynomial (dashed line), the parameters of which are obtained by fitting the calculated function $S(E_{\text{c.m.}})$ in the energy range $0.1 \leq E_{\text{c.m.}} \leq 0.3$ MeV. The experimental data for the astrophysical factor in the limit $E_{\text{c.m.}} \rightarrow 0$ taken from Refs. [3–7, 9], are labeled as “E03”, “T02”, “B01”, “G05”, “F12”, and “F15”, respectively. The astrophysical factor extracted from the Coulomb dissociation experiment [8] in the energy range $0.2 \text{ MeV} \leq E_{\text{c.m.}} \leq 0.6 \text{ MeV}$ is labeled as “M03”.

$E_0^{(A-1)}[\text{GSM}]$ denotes the GSM ground-state energy of ${}^8\text{B}$. S^{M1} is fairly small at low energies, but its contribution becomes comparable to S^{E1} in the region of $1/2^-_1$ resonance.

S^{E2} is significantly smaller than both S^{E1} and S^{M1} , as seen in Fig. 5. The $5/2^-_1$ resonance plays an important role in S^{E2} , while the contribution of $1/2^-_1$ resonance is small. A similar conclusion was made in the cluster model [11].

The total astrophysical factor S , which is a sum of S^{E1} , S^{M1} , and S^{E2} components, is shown in Fig. 6. In order to see the uncertainties brought by the E1 effective charge, we show in Fig. 6 results for S obtained using different

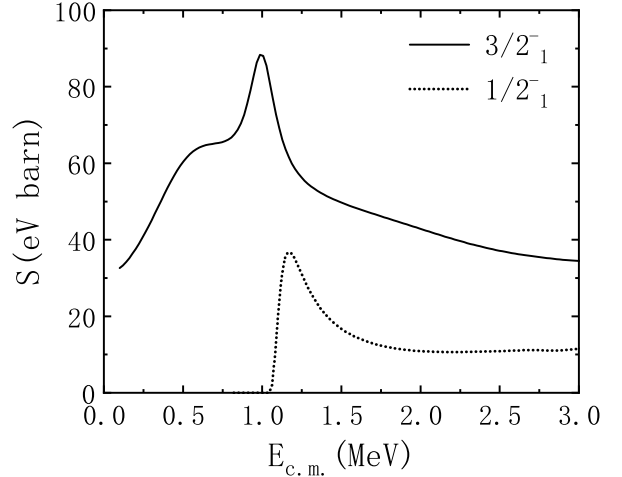


FIG. 7. The total astrophysical factor of the ${}^8\text{B}(p, \gamma){}^9\text{C}$ reaction. The capture reaction to the ground state of ${}^9\text{C}$ is shown by the solid line, and the capture to the first excited state, $1/2^-_1$, which is also the first resonant state, is given by the dotted line.

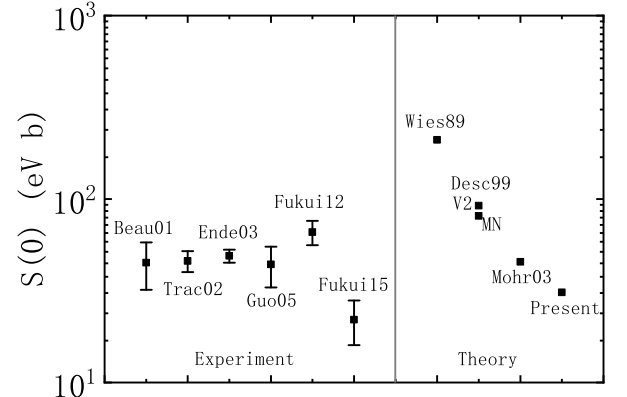


FIG. 8. Comparison between different experimental analyses [3–7, 9] and various theoretical calculations [1, 11, 12] of the total astrophysical S factor at $E_{\text{c.m.}} = 0$. The GSM-CC result is labeled as “Present”.

values of the scaling factor f_{E1} . The contribution to the astrophysical S factor from $E2$ transitions is so small compared to $E1$ and $M1$ transitions that the variation of $E2$ effective charges will not change the total S significantly, as seen in Fig. 5. Thus, we do not show results for different $E2$ effective charges. Experimental values for the astrophysical S factor in the limit $E_{\text{c.m.}} = 0$ [3–5, 9] seems to be smaller than the value obtained from a Coulomb-dissociation experiment [8] in range of proton energies $0.2 \text{ MeV} \leq E_{\text{c.m.}} \leq 0.6 \text{ MeV}$. This systematic feature of the data is reproduced by the GSM-CC calculation.

For a standard value of the effective charge $f_{E1} = 1.0$, the astrophysical factor calculated in the GSM-CC is slightly smaller than most of the existing data. For a slightly larger value of f_{E1} , a nice agreement with most

of the data can be reached. For $f_{E1} = 1.3$, the GSM-CC results are close to most of the upper limits of different experimental data.

In Figs. 2-6, only the astrophysical factors of the direct capture to the ground state of ${}^9\text{C}$ are given. Since the first excited state $1/2_1^-$ of ${}^9\text{C}$ is a resonance, its contribution to the total astrophysical S factor would be smaller [4, 5]. In Fig. 7, the results of the capture to the ground and the first excited state of ${}^9\text{C}$ are shown. It is seen that at around $E_{\text{c.m.}} = 1$ MeV, the explicit contribution of the capture to the $1/2_1^-$ resonance appears. This contribution has a small peak at around $E_{\text{c.m.}} = 1.2$ MeV and for higher energies has a stable contribution of about 20% to the total astrophysical S factor.

Most of the experimental analyses aimed at the astrophysical S factor in the limit $E_{\text{c.m.}} \rightarrow 0$. In Fig. 8, we collect values of $S(0)$ from various experimental analyses and theoretical studies and compare them with the GSM-CC result denoted as “Present”. The GSM-CC result shown in this figure is obtained for the standard value of the $E1$ effective charge ($f_{E1} = 1.0$) and the $E2$ effective charges from Ref. [37].

C. The astrophysical reaction rate

The ${}^8\text{B}(p, \gamma){}^9\text{C}$ reaction serves as an important step in the hot pp chain to produce the CNO nuclei, especially for temperatures $0.07 \leq T_9 \leq 0.7$ [1].

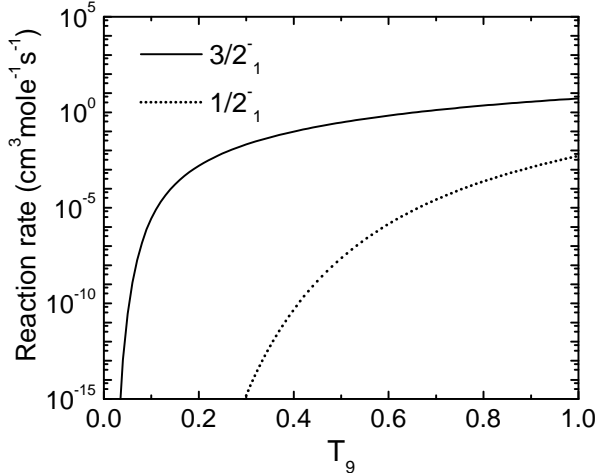


FIG. 9. The reaction rate of ${}^8\text{B}(p, \gamma){}^9\text{C}$ against the temperature T_9 calculated by GSM-CC. The solid line is the direct capture rate to the ground state $3/2_1^-$ and the dotted line is for the capture to the first excited resonance state $1/2_1^-$.

The astrophysical reaction rates against temperature for the ${}^8\text{B}(p, \gamma){}^9\text{C}$ reaction calculated by GSM-CC are given in Fig. 9, for the direct capture to the ground state and the resonant capture to the first excited state of ${}^9\text{C}$. As seen in the figure, the direct capture dominates the re-

action rates for the range of temperature of astrophysical interest, in agreement with previous studies [1].

The low reaction rates found in GSM-CC calculation imply that the most efficient temperature for the formation of ${}^9\text{C}$ is in the range of $0.1 \leq T_9 \leq 1$, i.e. significantly higher than the estimate given by Wiescher et al. [1] $0.07 \leq T_9 \leq 0.7$.

IV. CONCLUSIONS

In low-metallicity supermassive stars, ${}^8\text{B}(p, \gamma){}^9\text{C}$ reaction plays as an important role in the hot pp chain to produce the CNO nuclei [1]. When the temperature and the density are high, the proton capture of ${}^8\text{B}$ can be faster than its beta decay. Due to the experimental difficulties and theoretical uncertainties, the reaction rate of ${}^8\text{B}(p, \gamma){}^9\text{C}$ is not known precisely. The direct measurement of the reaction ${}^8\text{B}(p, \gamma){}^9\text{C}$ at $E_{\text{c.m.}} \sim 0$ is seemingly an impossible task. In the indirect measurements, It has been shown that the transformation from the observed ANC to the astrophysical $S(0)$ factor is quite uncertain due to strong model dependencies [3, 5-7].

In this work, we have applied the shell model for open quantum systems, the GSM-CC, to investigate both the proton radiative capture cross section of the reaction ${}^8\text{B}(p, \gamma){}^9\text{C}$ and the temperature dependence of its reaction rate. GSM-CC provides the unified theory of nuclear structure and reactions. In the present work, the Hamiltonian is given by the one-body core potential and the density-dependent two-body interaction whose parameters are adjusted to reproduce spectra and binding energies of ${}^8\text{B}$ and ${}^9\text{C}$. Once the Hamiltonian is fixed, the GSM-CC is used to calculate both spectra and cross-sections of the studied reaction using the same many-body approach.

The major contribution to the total astrophysical S factor is given by the $E1$ transitions. Especially, the transition from the proton s -wave to the p wave plays the leading role in $E1$ transitions. In agreement with the cluster model [10, 11], we find that the continuum states $J_i^\pi = 3/2^+, 5/2^+$ in ${}^9\text{C}$ play the major role in S^{E1} . Transitions from both these continua show a broad peak at around $E_{\text{c.m.}} = 0.6$ MeV. The $M1$ transitions contribute less to astrophysical S factor than $E1$, but it has a large peak around the energy of $1/2_1^-$ resonance. The contribution from $E2$ to S is much smaller than $E1$ and $M1$.

In our calculation, the direct capture to the ground state of ${}^9\text{C}$ dominates the astrophysical S factor. The capture to the $1/2_1^-$ resonance is less important but provides about 20% contribution at higher energies ($E_{\text{c.m.}} > 1$ MeV). Calculation of the temperature dependence of reaction rate shows that for the temperatures of the astrophysical interest, the direct capture has the leading contribution.

The existing experimental information about the astrophysical S factor suggest a sharp increase from $E_{\text{c.m.}} \approx 0$ [3-7, 9] to a region $0.2 \text{ MeV} \leq E_{\text{c.m.}} \leq 0.6 \text{ MeV}$ which

is probed in Coulomb-dissociation reaction [8]. This behavior is reproduced in the GSM-CC.

For a standard value $f_{E1} = 1$, the GSM-CC value for $S(0)$ is close to the lower limits of astrophysical factors determined in most indirect measurements [3–7, 9]. It is also significantly smaller than all previous theoretical predictions [1, 11, 12]. As a consequence, the critical temperature and density at which the proton capture reaction ${}^8\text{B}(p, \gamma){}^9\text{C}$ becomes faster than the beta decay is predicted by GSM-CC to be higher than previously ex-

pected.

V. ACKNOWLEDGEMENTS

This work has been supported by the National Natural Science Foundation of China under Grant Nos. U2067205, 12275081, 12175281, 11605054, and 12147219. G.X.D. and X.B.W. contributed equally to this work.

[1] M. Wiescher, J. Görres, S. Graff, L. Buchmann, and F.-K. Thielemann, *Astrophys. J.* **343**, 352 (1989).

[2] G.M. Fuller, S.E. Woosley, T.A. Weaver, *Astrophys. J.* **307**, 675 (1986).

[3] D. Beaumel, T. Kubo, T. Teranishi, H. Sakurai, S. Fortier, A. Mengoni, N. Aoi, N. Fukuda, M. Hirai, N. Imai, H. Iwasaki, H. Kumagai, H. Laurent, S.M. Lukyanov, J.M. Maison, T. Motobayashi, T. Nakamura, H. Ohnuma, S. Pita, K. Yoneda, M. Ishihara, *Phys. Lett. B* **514**, 226 (2001).

[4] B. Guo, Z. Li, W. Liu, X. Bai, G. Lian, S. Yan, B. Wang, S. Zeng, J. Su, and Y. Lu, *Nucl. Phys. A* **761**, 162 (2005).

[5] L. Trache, F. Carstoiu, A.M. Mukhamedzhanov, R.E. Tribble, *Phys. Rev. C* **66**, 035801 (2002).

[6] T. Fukui, K. Ogata, K. Minomo, and M. Yahiro, *Phys. Rev. C* **86**, 022801(R) (2012).

[7] T. Fukui, K. Ogata, and M. Yahiro, *Phys. Rev. C* **91**, 014604 (2015).

[8] T. Motobayashi, *Nucl. Phys. A* **719**, 65c (2003).

[9] J. Enders, T. Baumann, B.A. Brown, N.H. Frank, P.G. Hansen, P.R. Heckman, B.M. Sherrill, A. Stolz, M. Thoennessen, J.A. Tostevin, E.J. Tryggestad, S. Typel, M.S. Wallace, *Phys. Rev. C* **67**, 064301 (2003).

[10] P. Descouvemont, *Astrophys. J.* **405**, 518 (1993).

[11] P. Descouvemont, *Nucl. Phys. A* **646**, 261 (1999).

[12] P. Mohr, *Phys. Rev. C* **67**, 065802 (2003).

[13] N. Michel, W. Nazarewicz, M. Płoszajczak, and K. Bennaceur, *Phys. Rev. Lett.* **89**, 042502 (2002).
R. Id Betan, R. J. Liotta, N. Sandulescu, and T. Vertse, *Phys. Rev. Lett.* **89**, 042501 (2002).

[14] N. Michel, W. Nazarewicz, M. Płoszajczak, and J. Okołowicz, *Phys. Rev. C* **67**, 054311 (2003).

[15] N. Michel, W. Nazarewicz, M. Płoszajczak, and T. Vertse, *J. Phys. G: Nucl. Part. Phys.* **36**, 013101 (2009).

[16] Y. Jaganathan, N. Michel, and M. Płoszajczak, *Phys. Rev. C* **89**, 034624 (2014).

[17] K. Fossez, N. Michel, M. Płoszajczak, Y. Jaganathan, and R. M. Id Betan, *Phys. Rev. C* **91**, 034609 (2015).

[18] N. Michel, M. Płoszajczak, *Gamow Shell Model - The Unified Theory of Nuclear Structure and Reactions*, Lecture Notes in Physics, Vol. **983** (Springer, Cham, 2021), <https://doi.org/10.1007/978-3-030-69356-5>.

[19] T. Berggren, *Nucl. Phys. A* **109**, 265 (1968).

[20] R.M. Id Betan, *Phys. Lett. B* **730**, 18 (2014).

[21] S.M. Wang, W. Nazarewicz, *Phys. Rev. Lett.* **126**, 142501 (2021).

[22] A. Mercenne, N. Michel, and M. Płoszajczak, *Phys. Rev. C* **99**, 044606 (2019).

[23] G.X. Dong, N. Michel, K. Fossez, M. Płoszajczak, Y. Jaganathan, R.M. Id Betan, *J. Phys. G: Nucl. Part. Phys.* **44**, 045201 (2017).

[24] G.X. Dong, X.B. Wang, N. Michel, M. Płoszajczak, *Phys. Rev. C* **105**, 064608 (2022).

[25] Y. Suzuki and K. Ikeda, *Phys. Rev. C* **38**, 410 (1988).

[26] H. Furutani, H. Horiuchi, and R. Tamagaki, *Prog. Theor. Phys.* **60**, 307 (1978).

[27] H. Furutani, H. Horiuchi, and R. Tamagaki, *Prog. Theor. Phys.* **62**, 981 (1979).

[28] Y. Jaganathan, R. M. Id Betan, N. Michel, W. Nazarewicz and M. Płoszajczak, *Phys. Rev. C* **96**, 054316 (2017).

[29] <http://www.nndc.bnl.gov/nudat3/>, NuDat 3.0 database, National Nuclear Data Center, Brookhaven National Laboratory.

[30] K. W. Brown, R. J. Charity, J. M. Elson, W. Reviol, L. G. Sobotka, W. W. Buhro, Z. Chajecki, W. G. Lynch, J. Manfredi, R. Shane et al., *Phys. Rev. C* **95**, 044326 (2017).

[31] J. Hooker, G. V. Rogachev, E. Koshchiy, S. Ahn, M. Barbui, V. Z. Goldberg, C. Hunt, H. Jayatissa, E. C. Pollacco, B. T. Roeder, A. Saastamoinen, and S. Upadhyayula, *Phys. Rev. C* **100**, 054618 (2019).

[32] N.J. Stone, *Atomic Data and Nuclear Data Tables* **111-112**, 1 (2016).

[33] D.R. Tilley, J.H. Kelley, J.L. Godwin, D.J. Millener, J.E. Purcell, C.G. Sheu and H.R. Weller, *Nucl. Phys. A* **745**, 155 (2004).

[34] M. Huhta, P. F. Mantica, D. W. Anthony, B. A. Brown, B. S. Davids, R. W. Ibbotson, D. J. Morrissey, C. F. Powell, and M. Steiner, *Phys. Rev. C* **57**, 2790(R) (1998).

[35] B. A. Brown, A. Etchegoyen, N. S. Godwin, W. D. M. Rae, W. A. Richter, W. E. Ormand, E. K. Warburton, J. S. Winfield, L. Zhao and C. H. Zimmerman, MSU-NSCL report number 1289.

[36] R. E. Julies, W. A. Richter, and B. A. Brown, *S. Afr. J. Phys.* **15**, 35 (1992).

[37] A.G.M. van Hees, A.A. Wolters, P.W.M. Glaudemans, *Nuclear Physics A* **474**, 61 (1988).

[38] W. F. Hornyak, *Nuclear Structure* (Academic Press, New York, 1975).

[39] Y. K. Ho and C. Coceva, *J. Phys. G: Nucl. Phys.* **14**, S207 (1988).

[40] A. M. Lane and J. E. Lynn, *Nucl. Phys.* **17**, 563 (1961).

[41] B. J. Allen and A. R. Musgrave, *Advances in Nucl. Phys.* (Plenum, New York 1979) Vol. 10.

[42] W. V. Prestwich and T. J. Kenneth, (1984) *Phys. Rev. C* **30**, 392 (1984).

[43] B. Castel and Y. K. Ho, *Phys. Rev. C* **34**, 408 (1986).

[44] M. De Rydt, G. Neyens, K. Asahi and et. al., Physics Letters B **678**, 344 (2009).